ADVANCED BIOSYSTEMS
www.adv-biosys.com

Imaging with Optogenetically Engineered Living Cells as a Photodetector

Gongxin Li, Feifei Wang, Wenguang Yang, Wenxue Wang, Guangyong Li, Yuechao Wang, and Lianqing Liu**

Biosyncretic systems integrating biological components with electromechanical devices have recently become a promising technology, in which biological components are used as actuators or sensing elements with higher-level performance than artificial systems. Here, a biosyncretic imaging system using an optogenetically engineered living cell as a photodetector is shown. The photoresponsive properties of the cell, such as spectrum and response range, dynamic characteristics, are measured and indicate that the cell functions as an excellent photodetector. In the system, the cell is directly utilized to generate light-triggered ionic currents, which encode the spatial image information and therefore are used to reconstruct the scenes under the view based on compressive sensing. Imaging with the cell-based photodetector is successfully performed by acquiring high-definition images using the system. The system also displays function superiority to a commercial photodiode, such as wider dynamic responsivity range. This work represents a step toward directly imaging with living materials and paves a new road for the development of future on-body bionic devices.

1. Introduction

Biological components, such as cells and tissues, have evolved over millions of years within animals as nature's premier actuator and sensor with a higher-level performance that artificial devices currently cannot match. By integrating clusters of cells or tissues with electromechanical systems, complex biosyncretic systems can be possibly created with more advanced functions for potential applications in health recovery, security surveillance, and environment protection.[1–3]

Progress in the development of biological actuators and sensors empowered by living cells or tissues has been emerged in many reports. Through cells growing and self-assembling on micromechanical structures, Montemagno and coworkers assembled a muscle-powered microdevice that can be controllably released to enable free movement.[4] Mammalian cardiomyocytes were also assembled with the micro-electromechanical system (MEMS) to generate microdevices movement.[1,5] Using optogenetic tools, a light-controlled skeletal muscle bioactuator was made, which can generate up to 300 μN of active tension force under light stimulation;[6] optogenetically engineered cardiomyocytes were also used to activate a tissue-engineered soft robot via phototactically controlled locomotion.[7] Similarly, olfactory cells and epithelial tissues were used as sensing elements to build biosensors for their superior sensitivity.[8,9] Taste biosensors using taste cells and taste buds of mammalians were used to sense multiple taste signals elicited by different tastants.[10,11] These data show that mammalian cells and tissues are promising functional element candidates in biosyncretic systems for bioactuation and taste and olfactory sensing. However, there is almost no report on the biosyncretic imaging

Dr. G. X. Li, Prof. W. W. Wang, Prof. Y. C. Wang, Prof. L. Q. Liu
State Key Laboratory of Robotics
Shenyang Institute of Automation
Chinese Academy of Sciences
Shenyang 110016, China
E-mail: wangwenxue@sia.cn; lqliu@sia.cn

Dr. G. X. Li, Prof. W. W. Wang, Prof. Y. C. Wang, Prof. L. Q. Liu
Institutes for Robotics and Intelligent Manufacturing
Chinese Academy of Sciences
Shenyang 110016, China

Dr. G. X. Li, Prof. W. W. Wang, Prof. Y. C. Wang, Prof. L. Q. Liu
University of the Chinese Academy of Sciences
Beijing 100049, China

The ORCID identification number(s) for the author(s) of this article can be found under https://doi.org/10.1002/adbi.201800319.

DOI: 10.1002/adbi.201800319

Dr. G. X. Li
Key Laboratory of Advanced Process Control for Light Industry
(Ministry of Education)
Institute of Automation
Jiangnan University
Wuxi 214122, China

Dr. F. F. Wang
Department of Chemistry
Stanford University
Stanford, CA 94305, USA

Dr. W. G. Yang
School of Electromechanical and Automotive Engineering
Yantai University
Yantai 264005, China

Prof. G. Y. Li
Department of Electrical and Computer Engineering
University of Pittsburgh
PA 15213, USA

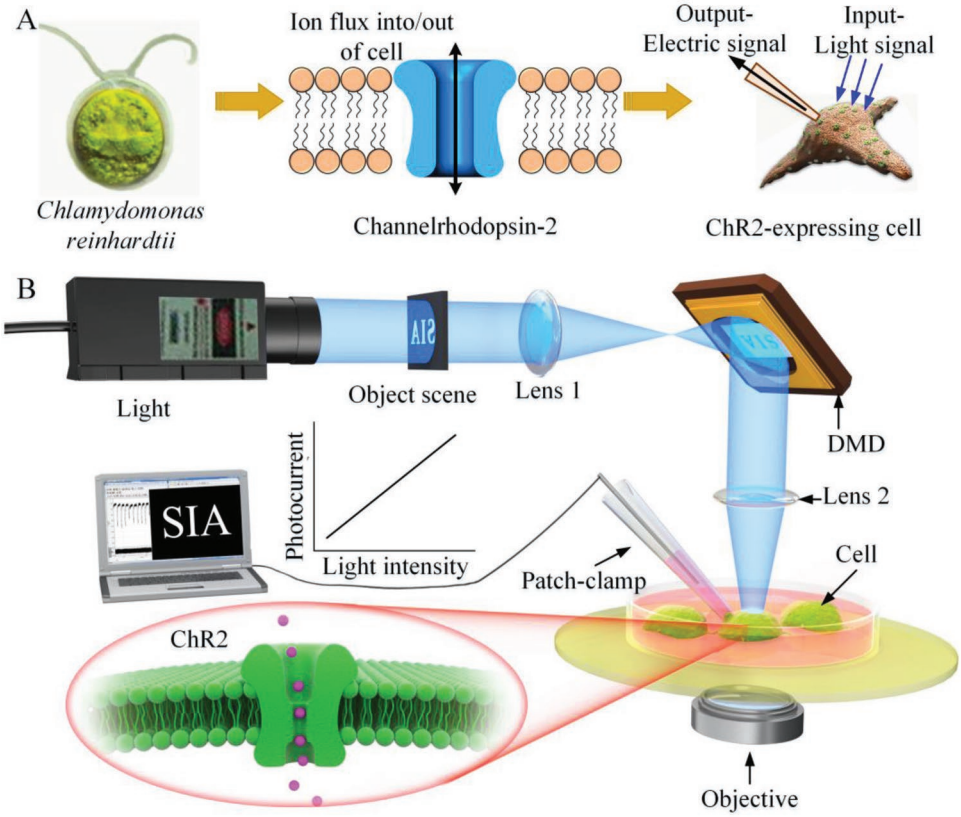

Figure 1. Conceptual design of the cell-based photodetector and biosyncretic imaging system. A) Established procedure of the cell-based photodetector. B) The system is composed of a single-pixel imaging system, an optogenetically engineered cell, and a patch clamp device. Variations in the input light intensity of an irradiated cell lead to varying ionic photocurrents, which are measured by the patch clamp device.

system which uses mammalian cells or tissues as biological photodetectors or light-sensing elements, although mammalian light-sensitive cells or tissues present some unique advantageous features superior to artificial imaging devices, such as the single-photon detection capability of retinal rods with ultrahigh light responsivity[12] and integration of the visual and infrared sensing capabilities of the rattlesnake.[13] Additionally, it has been reported that *Escherichia coli* was used to construct an engineered light sensor by optogenetic technique and "photograph" a light pattern as a high-definition chemical image,[14–16] but the bacterial system is essentially a light inducible transcription system to produce synthetic kinases allowing a lawn of bacteria to function as a biological film, and produces a static image for a prolonged exposure time whereas their setup lacks spatiality but exhibits acuteness.

In this study, we explore the feasibility of developing a cell-based photodetector using living light-sensitive cells and then construct a biosyncretic imaging system to test the performance of the developed photodetector. The light-sensitive cells used in this study are mammalian cells that are genetically modified to express channelrhodopsin-2 (ChR2), which is a light-sensitive protein discovered in the eyespot of the algae species, *Chlamydomonas reinhardtii*, and serve as sensory photoreceptors allowing the algae to identify optimal light condition for growth (**Figure 1**A). Therefore, the ChR2 is a promising candidate for the light-sensitive elements of cell-based photodetectors. Compared with the light sensor of the *E. coli* that converts the input light into a gene expression, the cell-based photodetector transforms the input light into ionic current, which is similar to the signal conversion manner of an electronic photodetector.

To test the performance of the cell-based photodetector that we designed (Figure 1A), a biosyncretic imaging system was constructed (Figure 1B). The system consists of three principal components: i) A cell-based photodetector, in which the cell is optogenetically engineered with a light-sensitive protein, ChR2; ii) a patch-clamp device, which provides a readout of the ionic photocurrent information of the cell under light irradiation; and iii) a single-pixel design based on the compressive sensing theory (detail is described in Text S1 in the Supporting information) that converts the spatial information of an object scene into time-varying light intensity signals to achieve high-resolution image.[17,18]

2. Results and Discussion

2.1. Photoresponsive Properties of the Cell-Based Photodetector

Living human embryonic kidney (Hek293) cells are modified to express the ChR2 for developing the cell-based photodetector. And the ChR2-expressing cells are also labeled with enhanced yellow fluorescent protein (EYFP) as shown in **Figure 2**A

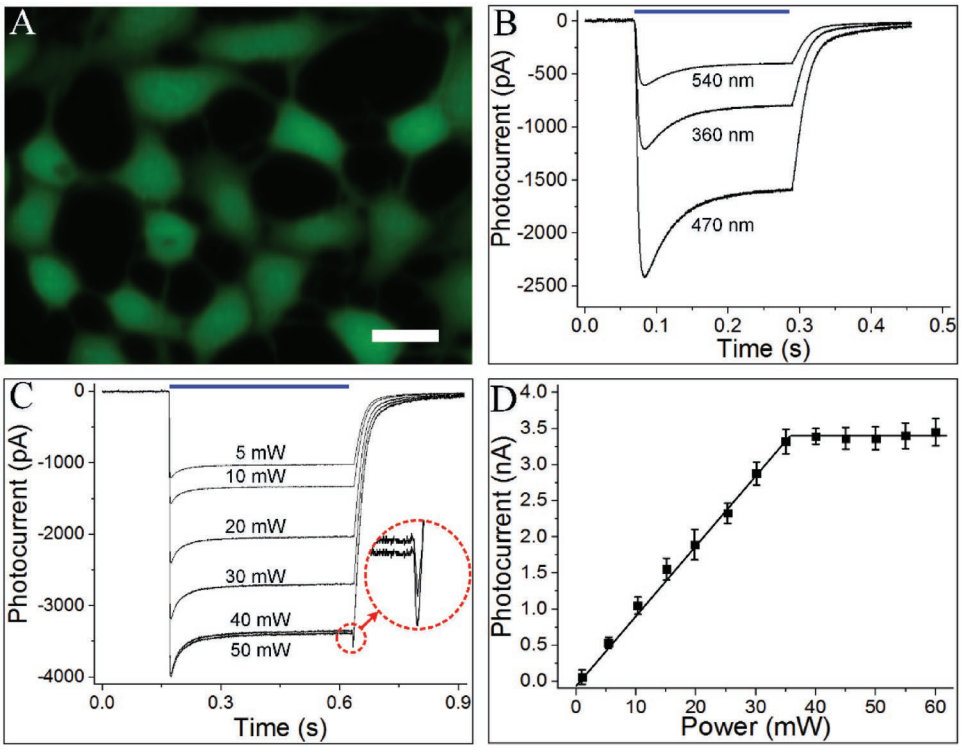

Figure 2. Photoresponsive characteristics of the cell-based photodetector. A) Fluorescence microscopy image of the Hek293 cell expressing ChR2-EYFP; the scale bar represents 40 µm. B) Photoresponse current of a cell to light of three different wavelengths, $n = 5$ cells. C) Photocurrent curves of a cell under incident light of different irradiation powers, $n = 7$ cells. D) Dynamic range of a cell, holding voltage −120 mV, $n = 6$ cells.

to discern whether the cells are successfully modified.[19,20] The opsin ChR2 is then incorporated with retinal, resulting in channel opening after the photons absorption and ion exchanging between the intracellular and extracellular compartments, which enabled the cell to generate photocurrents.[21] The biosyncretic imaging system provides a direct stimulus targeted to a single cell (Figure S1, Supporting Information) to activate the ion channels of ChR2. The experimental results indicate that the cells expressing ChR2 are triggered to generate photocurrents under light irradiation (Figure S2A, Supporting Information). The amplitude of the photocurrent is monotonically affected by the holding voltage of the patch clamp, as shown in Figure S2B in the Supporting Information. The experiments show that, for irradiation at the same light intensity, the amplitude of the photocurrent remains relatively stable and is larger over a longer period at a holding voltage of −120 mV than other holding voltages. As the holding potential becomes more negative (e.g., −160 mV or lower), a larger photocurrent can be generated, but stable photocurrent only preserves for a very short period. In addition, the cell displays significant adaptability, as shown in Figure S2C in the Supporting Information. When intermittent light of the same intensity irradiates a cell that had not been stimulated for several seconds, the first peak of the photocurrent is significantly larger than the subsequent current peaks; however, the subsequent peak photocurrent and all steady-state photocurrents are consistent. Therefore, the adaptability influences imaging accuracy, but the adaptability phenomenon can be eliminated by continuously irradiating the cell for about 500 ms and then maintaining the cell in the dark for 300 ms before imaging, as shown in Figure S2D in the Supporting Information.

To explore the spectra response range of the Hek293 cells expressing ChR2, light of three different wavelengths (360, 470, and 540 nm) were used to activate the opsin to generate photocurrents. The ChR2 opsin is activated by all three wavelengths and maximally activated by the blue light at 470 nm, as shown in Figure 2B. In addition, the photocurrent amplitude of the cell is also influenced by the incident light power. As shown in Figure 2C, the photocurrent amplitude is enhanced as the incident light power is increased and reaches saturation if the light power is large enough. As the incident light power is further increased, a second peak photocurrent is generated when illumination ceases, as shown by the red dotted circle in Figure 2C. The second peak photocurrent can be regarded as an indicator to discriminate whether the opsin reaches the saturation state. To examine the photoresponsivity characteristics of the cell, a pulsed 470 nm blue light with adjustable powers from 0 to 100 mW was used to consecutively activate the cell, and the corresponding photocurrents were recorded synchronously. As shown in Figure 2D, in terms of the peak values of the photoresponse current, the dynamic range of the cell is ≈0–37.8 ± 5.27 mW, and the cell photoresponsivity shows strong linearity within its dynamic range with respect to the incident light power. The calculated external responsivity of the cell is 94.77 ± 1.94 nA W^{-1}.

The photoresponsive stability is a crucial indicator for evaluating the performance of a photodetector during a long working time. To explore the stability of the cell-based photodetector,

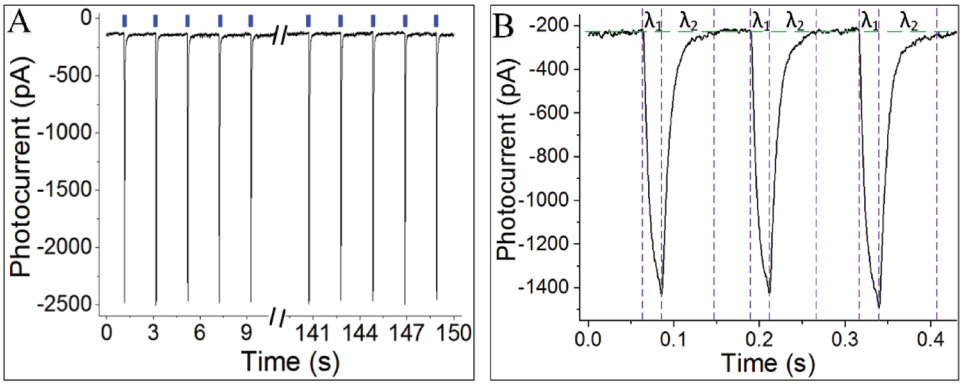

Figure 3. Photoresponsive stability and response rate of the cell as a photodetector. A) Photocurrent of a cell with a 10 ms flash light simulation with 2 s period over 150 s, $n = 6$ cells. B) Photoresponse time and rate of a cell, $n = 7$ cells.

0.01 s light pulses after 1.09 s dark period were used to simulate the cell, and the corresponding photocurrents were recorded, as shown in **Figure 3**A. The results show that the photocurrent remains very stable, and the statistical deviation of the peak photocurrent amplitude is 3% or less over 150 s. The high stability of the photocurrent implies that the cell state remains nearly constant during a certain period and ensures the imaging capability of the cell-based photodetector.

Moreover, the response rate of a photodetector directly determines the imaging rate. To explore the response rate of the cell triggered by photons, a 10 ms light pulse of 470 nm wavelength light was used to simulate the cell and the photocurrents before and after the light irradiation were recorded, as shown in Figure 3B. The response time for a light pulse stimulation contains an activation phase λ_1 and an inactivation phase λ_2. For the 10 light pulse stimulation, the activation time is 21.7 ± 0.76 ms, and the inactivation time is 55.6 ± 2.29 ms. The total photoresponse time for the 10 ms light pulse is $\approx 77.3 \pm 1.84$ ms, and the response rate is 12.9 s^{-1}.

2.2. Imaging Results of the Biosyncretic Imaging System

In the previous section, it was demonstrated that the photoresponsivity of a cell-based photodetector displays a good linearity with respect to the incident light power within its dynamic range and a high stability during a long working time. Therefore, the cell can act as a photodetector for imaging. In this section, the imaging capability of a single living cell was verified using the biosyncretic imaging system.

Five masks were used as object scenes for the imaging experiments with the biosyncretic imaging system using a single living cell as a photodetector (the system setup is shown in Figure S3 in the Supporting Information), as shown in **Figure 4**A–E. Images with resolution of 50×50 pixels obtained from the biosyncretic imaging system clearly show the object contour, as shown in Figure 4F–J. Through compressive sensing algorithm only 750 sensing points corresponding to 30% of the total pixels are needed to reconstruct the whole image[22] (the method of image reconstruction is described in the Text S2 in the Supporting Information). A commercial photodiode (OPT101, Texas Instruments Inc., USA) was also used as a photodetector in the single-pixel imaging system for comparison. The same object scenes were used in the experiments to reconstruct the image using the same compressive sensing algorithm, as shown in Figure 4K–O. Notably, the reconstructed images using the cell and the photodiode are very similar. The normalized observation vector of the single-pixel imaging system using the cell approximates that using the photodiode, as shown in Figure 4P, for object scene "A" (error comparisons for the other object scenes are shown in Figure S4 in the Supporting Information), and the element-wise differences between the two observation vectors are 3% or less. The results indicate that the imaging capability and effectiveness of the ChR2-expressing cell are close to those of the commercial photodiode. The imaging quality of the cell was quantitatively measured using the normalized mean squared error (NMSE, the calibrated method is described in Text S3 in the Supporting Information) and compared with that of the photodiode, as shown in Figure 4Q. The imaging NMSE using the cell for all object scenes are less than 0.2, demonstrating the imaging feasibility of a single living ChR2-expressing cell. The imaging NMSEs using the cell and the photodiode improves as the complexity of the object scenes increases because the reconstruction accuracy using a single photodetector (both the cell and the photodiode) is essentially limited by the compressive sampling of the single-pixel imaging system.

Compared with the photodiode (OPT101), the cell-based photodetector has an intrinsic advantage in imaging performance due to its wider dynamic range. The dynamic range of the photodiode was measured as ≈ 0–0.8 ± 0.11 mW and the external responsivity was calculated as 3.612 ± 0.16 A W^{-1}, as shown in Figure S5 in the Supporting Information. Therefore, the cell-based photodetector is superior to the photodiode in imaging over the dynamic range. The superiority of the cell-based photodetector to the photodiode was demonstrated by the imaging results of object scene "I" under two different incident light powers, 0.8 and 8 mW, the former of which is within the dynamic range of the cell and photodiode and the latter is within the dynamic range of the cell only. As shown in **Figure 5**, under the incident light power of 0.8 mW, both the cell and the photodiode (OPT101) are capable of imaging but the photodiode loses its imaging capability under the higher

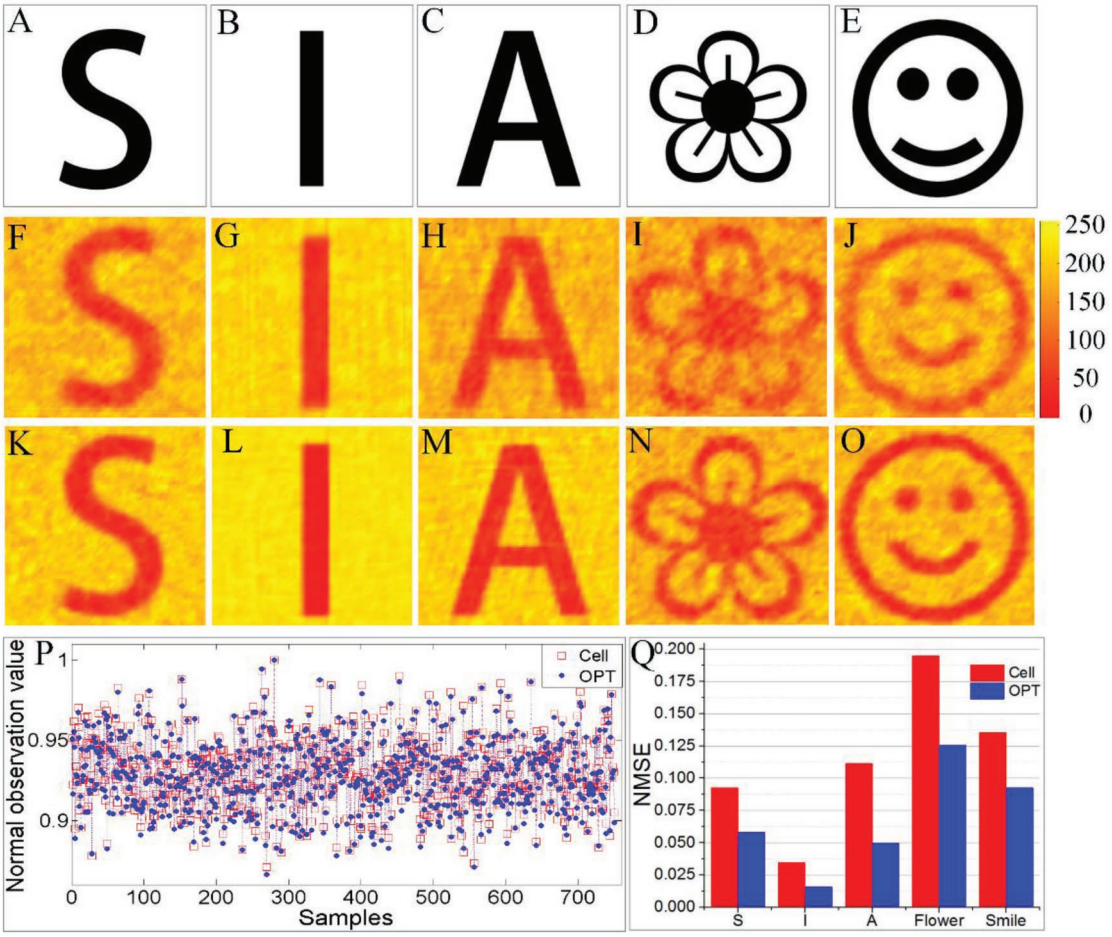

Figure 4. Imaging results. A–E) Object scenes ("S," "I," "A," "Flower," and "Smile") used to test the imaging feasibility of a single living ChR2-expressing cell. Only the spatial information corresponding to the white patches was sampled and carried by the light irradiated onto the cell. F–J) Images recovered using the single cell. K–O) Images recovered using the commercial photodiode (OPT101). P) Normalized observation vectors of the cell and photodiode, containing 750 elements corresponding to object scene "A." Q) Normalized mean squared errors of the images recovered using the cell and the photodiode for all object scenes.

incident light power of 8 mW, whereas the cell maintains its imaging capability.

3. Conclusion

In summary, we for the first time construct a biosyncretic imaging system based on an optogenetically modified light-sensitive cell. The analysis of photoresponsive properties of ChR2-expressing cells indicates that living light-sensitive cells can be excellent photodetectors with wide spectra and response ranges, and good dynamic characteristics. The imaging acquisition results for some object scenes validate the feasibility that the cell-based photodetector has the ability to acquire high-definition images. Moreover, the biosyncretic imaging system also may function in some manners that the imaging system with the conventional photodiode (OPT101) fails, such as taking a picture under a high light power condition. The physical prototype of the biosyncretic imaging system is a novel exploration in cell-based photodetector and represents a step toward a design of biosyncretic imaging systems. The concept of biosyncretic design disrupts the boundary between living media and nonliving artificial systems and has the great potential for the development of biosyncretic devices with a higher level of performance by directly utilizing the unique functional features of biological components instead of just physically mimicking. Because the triggered signals of the living medium are biologically natural and thus more biocompatible with respect to information communication, it will be easier and more compatibility for the human neural system to interface with such biosyncretic devices and decode the sensed information, demonstrating potential for future on-body bionic devices. Furthermore, recent advances in genetic tools[23] enable the genetic modification of cells and will lead to the functional improvement and customization of biosyncretic devices. These advantages allow for new trends in the future development of desired systems.

4. Experimental Section

Cell Preparation: Human embryonic kidney (Hek293) cells (Bought from the Cell bank of the Chinese Academy of Sciences, Shanghai, China)

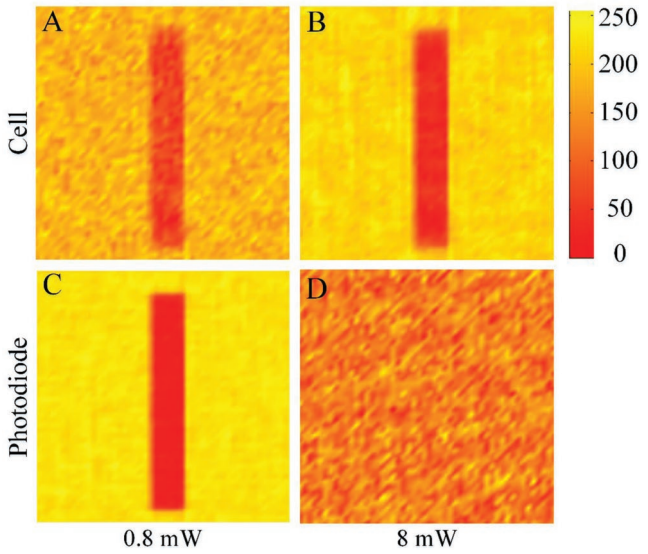

Figure 5. Imaging results under different incident light powers. A,B) Images recovered using the cell under different light powers (A—0.8 mW, B—8 mW). C,D) Images recovered using the photodiode under different light powers (C—0.8 mW, D—8 mW).

were grown in the culture medium, including high glucose Dulbecco's modified Eagle's medium (DMEM, Thermo Scientific) supplemented with 10% fetal bovine serum (FBS, ExCell Bio) and 1% penicillin-streptomycin (Thermo Scientific) solution, at 37 °C with 5% ambient CO_2 in a 9.6 cm^2 dish. The ChR2 plasmid used in this study was produced by a full-length (*chop2*-315) and a C terminally truncated *chop2* variant from a full-length cDNA template (GenBank accession no. AF461397) by PCR, using a proofreading polymerase (pfu, Promega) with primers containing BamHI and HindIII restriction sites. And, then, *chop2*-315 was additionally subcloned into pBK-CMV before expressed in Hek293 cells.[19] ≈4×10^5 cells per well were transfected using Transfection Reagent (Lipofectamine 2000, Sigma) according to the manufacturer's protocol. The cells were used 24 h after transfection, and *all-trans* retinal (1×10^{-6} M final concentration, Sigma) was added to the cultures 24 h before the experiment. Then, for electrophysiology experiments, the cells were seeded onto poly-D-Lysine (Sigma) coated glass coverslips.[24]

Electrophysiology: First, the external and internal recording solutions were prepared. The external recording solution contained: 140×10^{-3} M NaCl, 1×10^{-3} M $CaCl_2$, 2×10^{-3} M $MgCl_2$, and 10×10^{-3} M HEPES, pH 7.4; the internal recording solution included: 140×10^{-3} M NaCl, 5×10^{-3} M EGTA, 2×10^{-3} M $MgCl_2$, and 10×10^{-3} M HEPES, pH 7.4. Second, the ChR2-expressing cell were resuspended and dropped onto a glass slide covered with 0.1 mg mL^{-1} polylysine solution and incubated at 37 °C with 5% ambient CO_2 for ≈2 h.

The experiments were performed in a whole-cell configuration under voltage-clamp conditions (Axopatch 200B and DigiData 1440 interface; Axon Instruments) using pClamp 10.2. The patch-clamp pipettes were borosilicate glass capillaries (external diameter 1 mm and internal diameter 0.5 µm, Sutter Instrument Inc., USA) and the pipette resistance was ≈3.5–5 MΩ. The data were sampled at 10 kHz and processed with a low pass filter at 2 kHz. The seal resistance was greater than 1 GΩ, and the series resistance and capacitance must be compensated for in each recording. The membrane capacitance was ≈41.5 ± 2.1 pF. The cell used as a photodetector for imaging was selected if it was large, round, bulging and emitted bright fluorescence, as shown in Figure S6 in the Supporting Information.

Imaging Experiments: Because of the individual differences in cells, the dynamic range and response speed of the cell-based photodetector should be recalibrated before each image acquisition. To acquire the dynamic range of the cell-based photodetector, mirrors of the DMD were flipped onto the orientation of the cell-based photodetector, the incident light power was constantly increased and irradiated on the cell for 0.5 s and the photocurrent-response curve was measured, then, incident light power (P_{max}) corresponding to the critical point of the photocurrent saturation was determined by the existence of a second peak photocurrent when the light ceases. The P_{max} was the maximum power of the incident light used in this imaging process. To obtain the photocurrent response speed of the cell-based photodetector, the opsin was continuously activated by 0.5-second period flashes. The sum of the activation time and inactivation time was the photocurrent-response time for each light stimulus.

During the imaging process, a 10 ms light pulse of light was used to interrogate the cell-based photodetector every 100 ms. The light generator used in these experiments was a solid-state laser (470 nm, ≤ 200 mW), and the flashes of light were generated by the DMD.

Supporting Information

Supporting Information is available from the Wiley Online Library or from the author.

Acknowledgements

This work was supported by the National Key R&D Program of China (Grant No. 2018YFB1304700), the Natural Science Foundation of Jiangsu Province of China (Grant No. BK20180592), the National Natural Science Foundation of China (Grant Nos. 91748212, 61673372, 61433017, U1613220, U1813210, and 91848201), and the Key Research Program of Frontier Sciences, CAS (Grant No. QYZDB-SSW-JSC008).

Conflict of Interest

The authors declare no conflict of interest.

Keywords

biosyncretic imaging system, cell-based photodetector, optogenetically engineered cell

Received: November 28, 2018
Revised: June 3, 2019
Published online: June 21, 2019

[1] V. Chan, K. Park, M. B. Collens, H. Kong, T. A. Saif, R. Bashir, *Sci. Rep.* **2012**, *2*, 857.
[2] C. Wu, P. B. Lillehoj, P. Wang, *Analyst* **2015**, *140*, 7048.
[3] L. Ricotti, A. Menciassi, *Biomed. Microdevices* **2012**, *14*, 987.
[4] J. Xi, J. J. Schmidt, C. D. Montemagno, *Nat. Mater.* **2005**, *4*, 180.
[5] A. W. Feinberg, A. Feigel, S. S. Shevkoplyas, S. Sheehy, G. M. Whitesides, K. K. Parker, *Science* **2007**, *317*, 1366.
[6] R. Raman, C. Cvetkovic, S. G. Uzel, R. J. Platt, P. Sengupta, R. D. Kamm, R. Bashir, *Proc. Natl. Acad. Sci. USA* **2016**, *113*, 3497.
[7] S. J. Park, M. Gazzola, K. S. Park, S. Park, V. Di Santo, E. L. Blevins, J. U. Lind, P. H. Campbell, S. Dauth, A. K. Capulli, F. S. Pasqualini, S. Ahn, A. Cho, H. Y. Yuan, B. M. Maoz, R. Vijaykumar, J. W. Choi, K. Deisseroth, G. V. Lauder, L. Mahadevan, K. K. Parker, *Science* **2016**, *353*, 158.
[8] L. Du, C. Wu, H. Peng, L. Zhao, L. Huang, P. Wang, *Biosens. Bioelectron.* **2013**, *40*, 401.
[9] C. Wu, P. Chen, H. Yu, Q. Liu, X. Zong, H. Cai, P. Wang, *Biosens. Bioelectron.* **2009**, *24*, 1498.

[10] Q. Liu, D. Zhang, F. Zhang, Y. Zhao, K. J. Hsia, P. Wang, *Sens. Actuators, B* **2013**, *176*, 497.
[11] C. Wu, L. Du, L. Zou, L. Zhao, P. Wang, *Biomed. Microdevices* **2012**, *14*, 1047.
[12] D. A. Baylor, T. D. Lamb, K. W. Yau, *J. Physiol.* **1979**, *288*, 613.
[13] E. A. Newman, P. H. Hartline, *Science* **1981**, *213*, 789.
[14] J. J. Tabor, H. M. Salis, Z. B. Simpson, A. A. Chevalier, A. Levskaya, E. M. Marcotte, C. A. Voigt, A. D. Ellington, *Cell* **2009**, *137*, 1272.
[15] J. J. Tabor, A. Levskaya, C. A. Voigt, *J. Mol. Biol.* **2011**, *405*, 315.
[16] J. Fernandez-Rodriguez, F. Moser, M. Song, C. A. Voigt, *Nat. Chem. Biol.* **2017**, *13*, 706.
[17] G. Li, W. Wang, Y. Wang, W. Yang, L. Liu, *Opt. Express* **2016**, *24*, 400.
[18] G. Li, J. Yang, W. Yang, Y. Wang, W. Wang, L. Liu, *Remote Sens.* **2017**, *9*, 619.
[19] G. Nagel, T. Szellas, W. Huhn, S. Kateriya, N. Adeishvili, P. Berthold, D. Ollig, P. Hegemann, E. Bamberg, *Proc. Natl. Acad. Sci. USA* **2003**, *100*, 13940.
[20] G. Li, J. Yang, Y. Wang, W. Wang, L. Liu, *Nanoscale* **2018**, *10*, 21046.
[21] F. Zhang, J. Vierock, O. Yizhar, L. E. Fenno, S. Tsunoda, A. Kianianmomeni, M. Prigge, A. Berndt, J. Cushman, J. Polle, J. Magnuson, P. Hegemann, K. Deisseroth, *Cell* **2011**, *147*, 1446.
[22] G. Li, W. Wang, Y. Wang, S. Yuan, W. Yang, N. Xi, L. Liu, *IEEE Trans. Nanotechnol.* **2015**, *14*, 837.
[23] J. D. Sander, J. K. Joung, *Nat. Biotechnol.* **2014**, *32*, 347.
[24] G. Li, J. Yang, W. Yang, F. Wang, Y. Wang, W. Wang, L. Liu, *Nanoscale* **2018**, *10*, 2285.

